# FERM-dependent E3 ligase recognition is a conserved mechanism for targeted degradation of lipoprotein receptors

Anna C. Calkin[a,b,1], Benjamin T. Goult[c,1], Li Zhang[a,b], Louise Fairall[c], Cynthia Hong[a], John W. R. Schwabe[c,2], and Peter Tontonoz[a,b,2]

[a]Howard Hughes Medical Institute and [b]Department of Pathology and Laboratory Medicine, David Geffen School of Medicine at University of California, Los Angeles, CA 90095; and [c]Henry Wellcome Laboratories of Structural Biology, Department of Biochemistry, University of Leicester, Leicester LE1 9HN, United Kingdom

Edited by Michael S. Brown, University of Texas Southwestern Medical Center, Dallas, TX, and approved October 27, 2011 (received for review July 18, 2011)

**The E3 ubiquitin ligase IDOL (inducible degrader of the LDL receptor) regulates LDL receptor (LDLR)-dependent cholesterol uptake, but its mechanism of action, including the molecular basis for its stringent specificity, is poorly understood. Here we show that IDOL uses a singular strategy among E3 ligases for target recognition. The IDOL FERM domain binds directly to a recognition sequence in the cytoplasmic tails of lipoprotein receptors. This physical interaction is independent of IDOL's really interesting new gene (RING) domain E3 ligase activity and its capacity for autoubiquitination. Furthermore, IDOL controls its own stability through autoubiquitination of a unique FERM subdomain fold not present in other FERM proteins. Key residues defining the IDOL–LDLR interaction and IDOL autoubiquitination are functionally conserved in their insect homologs. Finally, we demonstrate that target recognition by IDOL involves a tripartite interaction between the FERM domain, membrane phospholipids, and the lipoprotein receptor tail. Our data identify the IDOL–LDLR interaction as an evolutionarily conserved mechanism for the regulation of lipid uptake and suggest that this interaction could potentially be exploited for the pharmacologic modulation of lipid metabolism.**

The LDL receptor (LDLR) is a cell membrane protein that mediates uptake of LDL cholesterol and is a major determinant of plasma lipoprotein levels (1–3). The primary transcriptional regulator of LDLR is the transcription factor SREBP-2 (sterol regulatory element-binding protein 2) (4). A major posttranslational regulator is PCSK9 (proprotein convertase subtilisin/kexin type 9), a secreted factor that binds to the extracellular domain of the LDLR (5–7). We recently identified the really interesting new gene (RING) domain E3 ubiquitin ligase IDOL (inducible degrader of the LDLR) as an additional posttranslational mechanism for modulation of the LDLR pathway (8). Induction of IDOL by the sterol-responsive nuclear receptor liver X receptor (LXR) represents a complementary pathway for feedback inhibition of cellular cholesterol uptake.

Although it is clear that increased expression of IDOL leads to ubiquitination of the LDLR and subsequent degradation, the mechanism by which this is accomplished remains to be elucidated. IDOL is unusual among E3 ligases in that it affects the degradation of a very small number of proteins. Our data suggest that the closely related family members LDLR, very-low-density lipoprotein receptor (VLDLR), and apolipoprotein E receptor 2 (ApoER2) are the only proteins targeted by IDOL. The basis for this remarkable specificity is unknown. Here we define the molecular basis for IDOL target recognition, and we provide evidence that specific targeting of membrane receptors by binding of the IDOL FERM domain underlies a conserved mechanism for the regulation of lipoprotein uptake.

## Results

**FERM-Dependent Target Recognition.** To determine the mechanism whereby IDOL triggers specific degradation of LDLR, ApoER2, and VLDLR, we performed structure–function analysis. IDOL contains two distinct domains: a C-terminal RING domain, defining it as an E3 ligase; and an N-terminal FERM (Band 4.1, ezrin-radixin-moesin) domain, a putative protein–protein interaction motif (Fig. 1*A*). The IDOL FERM domain comprises a tridomain structure common to FERM proteins (9). However, sequence alignments of IDOL with other FERM domain-containing proteins revealed that IDOL contains an apparent insertion within the F3 domain (residues 215–272, designated subdomain F3b; Fig. S1 *A*–*C*). Secondary structure prediction suggested a duplication of the C-terminal portion of the F3 phosphotyrosine binding (PTB) domain (i.e., the F3b and F3c subdomains share significant homology).

Functional analysis indicated that each FERM subdomain was required for IDOL-mediated degradation, because deletion of any of them abrogated the ability of IDOL to promote LDLR degradation in an HEK293T cell cotransfection assay (Fig. S1*D*). We generated two structural homology models of the IDOL FERM with different F3 subdomain assignments using PHYRE: 1–344 with the deletion of residues 215–272, and 1–276 lacking residues 277–344. These two regions are denoted F3a:F3c and F3a:F3b, respectively (Fig. 1*A*). We used these alternative models to generate predictions of residues important for the recognition of the LDLR cytoplasmic tail, on the basis of the known mode of interaction between the Talin FERM domain and the β-integrin cytoplasmic tail (Fig. 1*A*).

To test the function of these predicted protein–protein interaction surfaces, we introduced designed mutations. Because there are no antibodies capable of efficiently detecting native IDOL protein, and because epitope tags have the potential to affect protein function, we performed our initial analyses using native IDOL constructs. Mutation of the key amino acids denoted in Fig. 1*A* demonstrated that Y265 and T269, which reside in the F3b subdomain, were especially important for IDOL-induced LDLR degradation (Fig. 1*B*). Indeed, the activity of Y265A was comparable to that of a ubiquitination-defective RING mutant (C387A) (8, 10). Q232A showed partial activity when lower levels of IDOL were used. Mutations of M285 and Y323, which lie in the F3c subdomain, had only modest effects.

Using a biotin-labeling approach (11), we found that the T269R and Y265A mutants were defective in their ability to clear LDLR from the plasma membrane (Fig. S2*A*). To test the functional consequence of these mutations, we assayed cellular

Author contributions: A.C.C., B.T.G., C.H., J.W.R.S., and P.T. designed research; A.C.C., B.T.G., L.Z., L.F., and C.H. performed research; A.C.C., B.T.G., L.Z., L.F., C.H., J.W.R.S., and P.T. analyzed data; and A.C.C., B.T.G., J.W.R.S., and P.T. wrote the paper.

The authors declare no conflict of interest.

This article is a PNAS Direct Submission.

Freely available online through the PNAS open access option.

[1]A.C.C. and B.T.G. contributed equally to this work.

[2]To whom correspondence may be addressed. E-mail: john.schwabe@le.ac.uk or ptontonoz@mednet.ucla.edu.

This article contains supporting information online at www.pnas.org/lookup/suppl/doi:10.1073/pnas.1111589108/-/DCSupplemental.

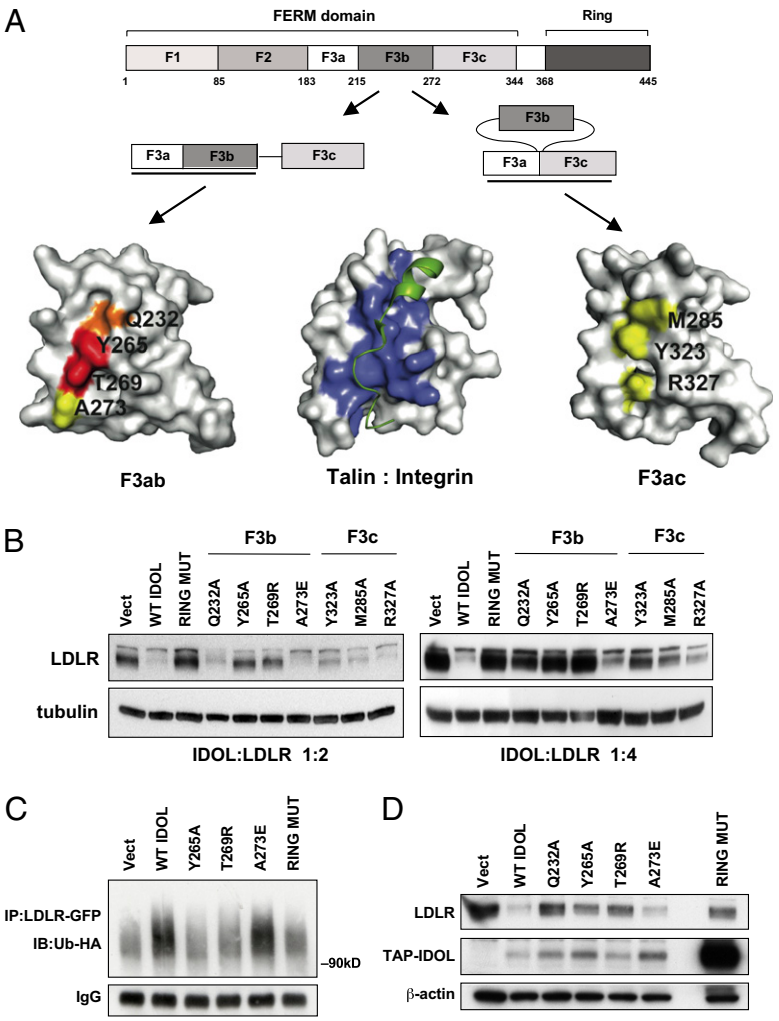


**Fig. 1.** The FERM 3b subdomain of IDOL is critical for LDLR recognition. (*A*) Domain structure of IDOL and potential configurations of FERM F3 domain; residue numbers indicate domain boundaries (*Upper*); computer-generated 3D modeling of IDOL denoting surface residues available for target interaction in either conformation; F3ab 1–276 lacking residues 277–344 (*Left*) and F3ac 1–344 with the deletion of residues 215–272 (*Right*) based on Talin interaction with integrin (*Center*). (*B*) Immunoblot of HEK293T whole-cell lysates after overnight cotransfection with LDLR and IDOL WT, F3b, or F3c subdomain mutants. (*C*) Analysis of ubiquitinated LDLR in HEK293T lysates after cotransfection with GFP-LDLR, HA-ubiquitin, and IDOL expression plasmids. Proteins were immunoprecipitated with anti-GFP antibody followed by immunoblotting for HA-ubiquitin. (*D*) Immunoblot of HEK293T lysates after cotransfection with LDLR and TAP-IDOL constructs.

uptake of fluorescently labeled LDL. As expected, the inhibitory activity of T269R on LDL uptake was dramatically reduced compared with WT, and Q232A exhibited a partial defect (Fig. S2*B*). We also stably expressed F3b mutants in IDOL$^{-/-}$ mouse embryonic fibroblasts (MEFs). Stable expression of WT IDOL was associated with lower LDLR expression than control IDOL$^{-/-}$ MEFs (Fig. S2*C*). By contrast, cells stably expressing Q232A, Y265A, or T269R IDOL all exhibited greater LDLR abundance. Furthermore, we observed reduced uptake of LDL particles in IDOL$^{-/-}$ MEFs expressing WT compared with those expressing RING mutant, Q232A, Y265A, or T269R (Fig. S2*D*).

We predicted that the lack of LDLR degradation associated with F3b mutants would correlate with reduced ubiquitination. The data in Fig. 1*C* revealed reduced ubiquitination of the LDLR in the presence of Y265A and T269R compared with WT IDOL. To rule out differences in the expression of the various mutants used above, we repeated our analysis using TAP-tagged IDOL constructs. Y265A and T269R again showed markedly reduced ability to degrade the LDLR (Fig. 1*D*). Furthermore, the observation that all of the FERM domain mutants in Fig. 1*D* showed WT stability indicated that the ligase activity of these mutants was intact, because mutations that affect intrinsic E3 ligase activity stabilize IDOL owing to loss of autoubiquitination (8).

**Conserved WxxKNxxSI/MxF Sequence as an IDOL Recognition Motif.** Only LDLR, VLDLR, and ApoER2 seem to be targeted by IDOL. Thus, these proteins must harbor a specific recognition sequence. To identify the IDOL degradation motif, we combined sequence analysis and structural modeling (Fig. 2 *A* and *B*). We hypothesized that the FERM domain might bind directly to lipoprotein receptor tails and generated a homology model of the FERM domain (1–276) with PHYRE using the structure of the Protein 4.1R core domain [Protein Data Bank (PDB) ID: 1gg3]. The two proteins are 27% identical and 47% similar in the modeled region. The LDLR cytoplasmic tail was docked with reference to the structures of Talin in complex with layillin, PIPKI-γ, and integrin-β1D (PDB IDs: 2k00, 2G35, and 3G9W, respectively) (12–14). The resulting model suggests that W813, I821, and F823 in the LDLR tail should be key residues mediating the interaction with the F3b domain (Fig. 2*B*). Interestingly, the IDOL model reveals a pocket adjacent to residues Y265 and T269 that is not present in other PTB domains. F823 at position −5 relative to the NPVY motif (where Y is position 0) on the LDLR tail is positioned optimally to fit into this pocket. Another key determinant suggested from the model was the interaction of LDLR I821 with a nonpolar surface on the FERM domain. Finally, W813 is also optimally positioned to interact with another large nonpolar FERM surface.

In support of our model, site-directed mutagenesis of the LDLR identified a series of conserved amino acids important for IDOL-mediated degradation (Fig. 3*A* and Fig. S3*A*). W813A, F823A, and I821E were resistant to degradation, whereas K816A, N817A, and S820D were partially resistant. Mutation of other conserved residues in the LDLR tail, including each residue in the NPVY internalization motif, did not inhibit degradation. A chimeric protein in which LDLR was fused to GFP distal to F823 retained its ability to be degraded by IDOL, but a fusion after I821 was resistant, indicating that the sequences

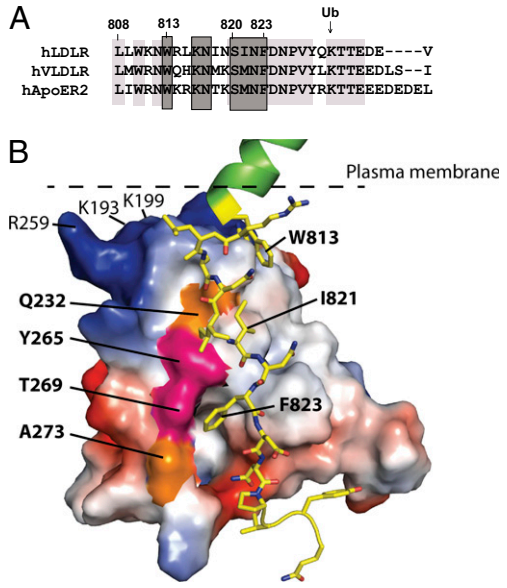


**Fig. 2.** Model for IDOL FERM–LDLR tail interaction. (*A*) Sequence alignment of IDOL targets, with key residues for IDOL recognition highlighted in dark gray; the ubiquitination (Ub) site is indicated by the arrow; homologous residues are shaded in light gray. (*B*) 3D model of IDOL–LDLR interaction highlighting critical residues in the LDLR tail and F3b domain; pink residues indicate those predicted to be most important; orange residues indicate those predicted to be somewhat important; the plasma membrane is marked by a dotted line. The electrostatic surface of IDOL is shown with basic surfaces in blue and acidic surfaces in red.

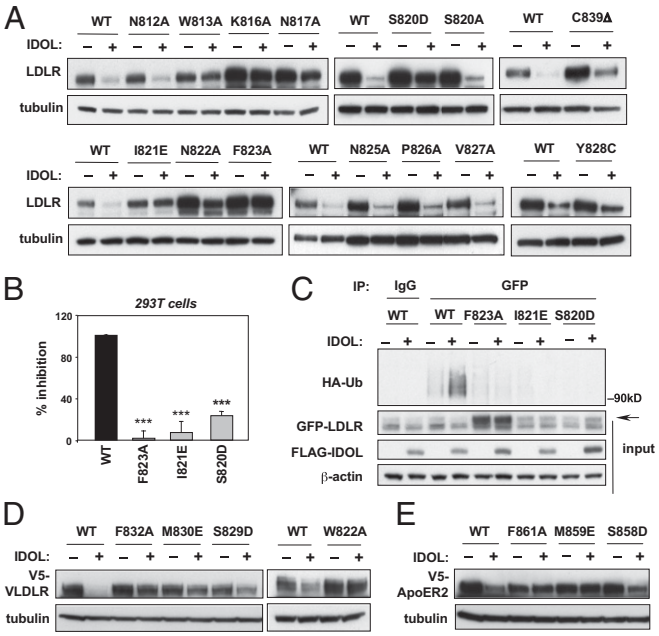


**Fig. 3.** A conserved IDOL recognition sequence in lipoprotein receptor tails. (*A*) Immunoblot of HEK293T lysates after cotransfection with IDOL and LDLR constructs. (*B*) IDOL-dependent inhibition of DiI-LDL uptake in HEK293T cells transfected with IDOL and LDLR constructs before DiI-LDL (4 μg/mL) uptake for 1 h at 37 °C. Data are represented as percentage inhibition and expressed as mean ± SEM, performed in triplicate. The inhibitory activity of WT IDOL on WT LDLR was assigned a value of 100%. ***$P < 0.001$ vs. WT LDLR. (*C*) Analysis of ubiquitinated LDLR in HEK293T lysates after cotransfection with HA-ubiquitin, FLAG-IDOL, and GFP-LDLRs. Proteins were immunoprecipitated with anti-GFP or IgG, followed by immunoblotting for HA-ubiquitin. (*D*) Immunoblot of HEK293T lysates after cotransfection with IDOL and V5-VLDLRs. (*E*) Immunoblot of HEK293T lysates after cotransfection with IDOL and V5-ApoER2s.

upstream of and including F823 are sufficient for IDOL targeting (Fig. S3*B*). Transfection of mutated LDLR constructs into 293T cells revealed that resistance to IDOL-dependent degradation also translated to resistance to IDOL-dependent inhibition of LDL uptake (Fig. 3*B*).

We next endeavored to link the WxxKNxxSI/MxF motif to ubiquitination. Mutations at F823, I821, or S820 led to reduced ubiquitination by IDOL (Fig. 3*C*), consistent with our degradation results. To verify the importance of the WxxKNxxSI/MxF motif for LDLR degradation in response to the endogenous LXR-IDOL pathway, we stably expressed LDLR constructs in LDLR$^{-/-}$ MEFs. Treatment with the LXR agonist GW3965, an inducer of IDOL expression (8), reduced the expression of WT LDLR and inhibited LDL uptake but had little effect on any of the LDLR mutants (Fig. S3*C*).

Interestingly, W813, F823, and S820 are conserved across all three IDOL targets (Fig. 2*A*). In place of LDLR I821, VLDLR and ApoER2 have a conservative methionine substitution. We investigated the importance of these residues for degradation of VLDLR and ApoER2. Mutation of the tryptophan, phenylalanine, or the methionine rendered the receptor resistant to degradation, confirming that these amino acids are part of the recognition motif (Fig. 3 *D* and *E*). Mutation of the serine equivalent to S820 had a minor effect on VLDLR degradation and little effect on ApoER2 degradation.

**Key Residues in the IDOL FERM Domain and LDLR Are Functionally Conserved.** Given that integral physiological processes tend to be conserved through evolution, we examined IDOL sequences across species. The most important residues for LDLR recognition in the IDOL F3b subdomain are conserved in vertebrates and in the insect IDOL homolog DNR1 (Fig. 4*A*). We further demonstrated that the function of these residues was also conserved. DNR1 degraded human LDLR when expressed in 293T cells (15). However, DNR1 point mutations in the residues corresponding to human Y265 and T269 (Y405 and T409) were associated with reduced LDLR degradation (Fig. 4*B*). Their reduced ability to inhibit LDL uptake further confirmed the functional importance of these residues for regulation of cholesterol uptake (Fig. 4*C*).

Sequence alignment also revealed conservation of the WxxKNxxSI/MxF motif in LDLRs across vertebrate species (Fig. 4*D*). Remarkably, this sequence is largely conserved in the lipophorin receptor (LpR), the major lipoprotein carrying receptor in insects. IDOL promoted the degradation of LpR, indicating that LpR can indeed be recognized by the FERM domain (Fig. 4*E*). Furthermore, the residue corresponding to LDLR F823 (F992) was critical for IDOL-dependent degradation. Thus, key aspects of the IDOL mechanism of action are conserved through evolution. However, IDOL was substantially less potent at degrading LpR compared with LDLR (Fig. 4*E*). This may reflect the fact that the key upstream tryptophan residue (LDLR W813) is not conserved in insects.

**FERM 3c Subdomain Controls IDOL Stability.** The FERM domain of IDOL contains a region of duplicated sequence (F3c) that is not present in other FERM domains. We identified a series of lysine residues in this region that influence IDOL protein stability (Fig. 5*A*). K293R and K309R mutants had the greatest influence on IDOL abundance (Fig. 5*B*), and these are also the most highly conserved of the lysines in F3c. Subsequent compound mutants were also associated with increased LDLR degradation (Fig. 5*C*). MG-132 had little effect on protein levels of the 4X mutants, further confirming that they were no longer undergoing proteasomal degradation (Fig. S4). Moreover, mutation of lysine residues in the F3c subdomain strongly reduced IDOL autoubiquitination (Fig. 5*D*).

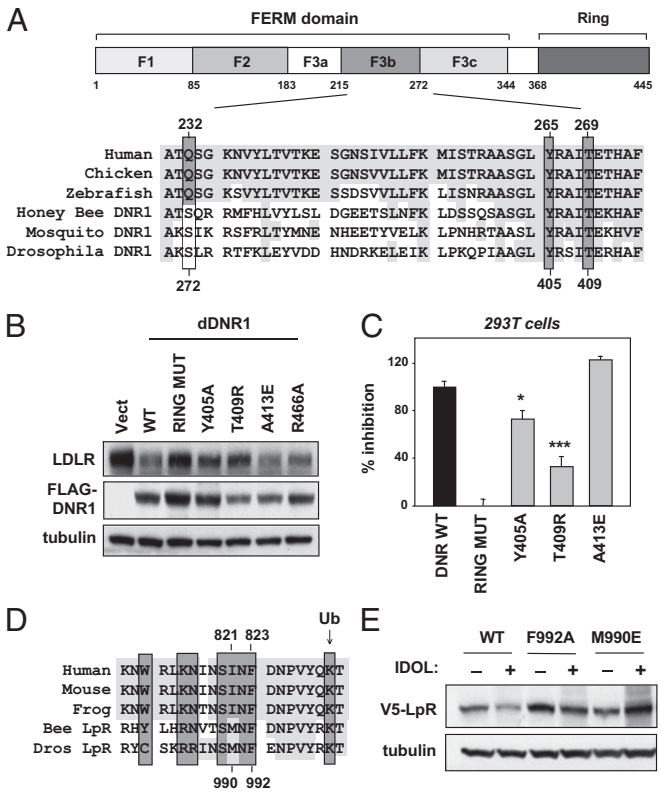


**Fig. 4.** IDOL LDLR structure–function relationships are conserved in insect orthologs. (*A*) Sequence alignment of the IDOL F3b domain and DNR1; homologous residues are shaded in gray. (*B*) Immunoblot of HEK293T lysates after cotransfection with LDLR and FLAG-DNR1 constructs. (*C*) DNR1-dependent inhibition of DiI-LDL uptake in HEK293T cells transfected with LDLR and DNR1 constructs, followed by incubation with DiI-LDL (4 μg/mL) for 1 h at 37 °C. Data represented as percentage inhibition and expressed as mean ± SEM, performed in triplicate. The inhibitory activity of WT DNR1 on WT LDLR was assigned a value of 100%. $*P < 0.05$, $***P < 0.001$. (*D*) Sequence alignment of the cytoplasmic tails of the LDLR and its insect homolog, LpR, with key residues for IDOL recognition and ubiquitination highlighted; homologous residues are shaded in gray. (*E*) Immunoblot of HEK293T lysates after cotransfection with IDOL and V5-LpR constructs.

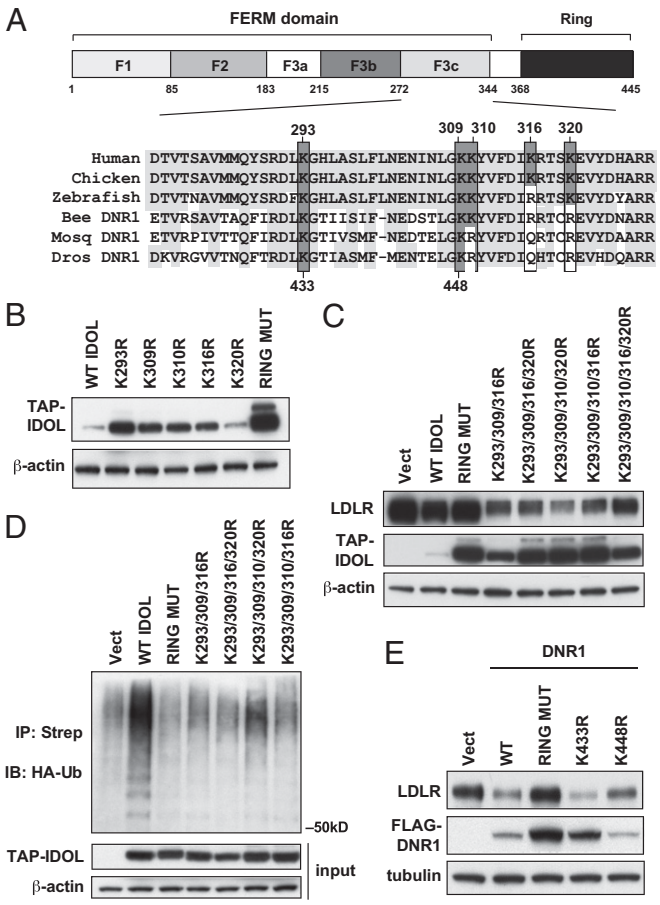


**Fig. 5.** The FERM 3c subdomain of IDOL is required for autoubiquitination. (*A*) Sequence alignment of the F3c subdomain of IDOL/DNR1 demonstrating conservation of key lysine residues across species; homologous residues are shaded in gray. (*B*) Immunoblot of HEK293T lysates after cotransfection with TAP-IDOL constructs. (*C*) Immunoblot of HEK293T lysates after cotransfection with LDLR and TAP-IDOL constructs. (*D*) IDOL autoubiquitination in HEK293T cell lysates after transfection with TAP-IDOL constructs and HA-ubiquitin. Cells were incubated with MG-132 for 5 h before harvest. TAP-IDOL was immunoprecipitated overnight with streptactin beads, followed by immunoblotting for HA-ubiquitin. (*E*) Immunoblot of HEK293T lysates after cotransfection with LDLR and FLAG-DNR1 constructs.

Interestingly, *Drosophila* DNR1 also seems to undergo autodegradation (Fig. 5*E*). Mutation of the conserved lysine corresponding to IDOL K293 (K433R) increased DNR1 protein stability and increased LDLR degradation, consistent with reduced capacity for autoubiquitination (Fig. 5*E*). Thus, the function of the F3c regulatory domain for IDOL protein turnover also seems to be evolutionarily conserved.

**Membrane Context Is Critical for IDOL-Dependent LDLR Degradation.** Interestingly, IDOL was unable to promote the degradation of a fusion protein consisting of the LDLR cytoplasmic domain fused to GFP (Fig. S5). This suggested that IDOL–membrane interaction might be required for efficient LDLR recognition. We therefore analyzed the ability of IDOL to associate with membrane fractions from 293T cells transfected with LDLR. The abundance of WT, Q232A, and T269R IDOL proteins in total cell lysates was similar (Fig. 6*A*). However, in membrane fractions, we readily detected the presence of WT IDOL in cells transfected with LDLR but not those transfected with vector alone. Furthermore, Q232A and Y265R, which were defective in LDLR degradation, showed reduced ability to associate with the membrane fraction, even in the presence of more LDLR in the membrane (due to lack of degradation).

To further explore the IDOL–membrane–LDLR interaction we used in vitro assays that are able to detect weak but relevant protein–lipid and protein–peptide interactions. Structural modeling suggested that the FERM domain has a high proportion of positively charged residues, predominantly on the face of the protein predicted to be proximal to the membrane (Fig. 6*B*). To determine whether there was a direct interaction between the IDOL FERM domain and the membrane, we performed vesicle cosedimentation assays (Fig. 6*C*). In the absence of vesicles or in the presence of neutral phosphatidylcholine vesicles, the FERM remained in the supernatant fraction. However, increasing the negative charge content of the vesicles to 100% phosphatidylserine caused 80% of WT IDOL to precipitate with the vesicles. Interestingly, the interaction of IDOL with these vesicles was considerably weaker than that of the Talin FERM domain (Fig. 6*C*). This is suggestive of a more transient IDOL–LDLR–membrane interaction and is consistent with the requirement for the LDLR tail in the cell-based assays. To confirm that membrane-facing FERM residues were important for LDLR degradation, we performed cosedimentation and LDLR degradation assays. An IDOL R73E/K75E mutant (domain F1) showed a partial reduction in LDLR degradation activity, and a R193E/K199E/R259E mutant (domain F3) construct showed a prominent

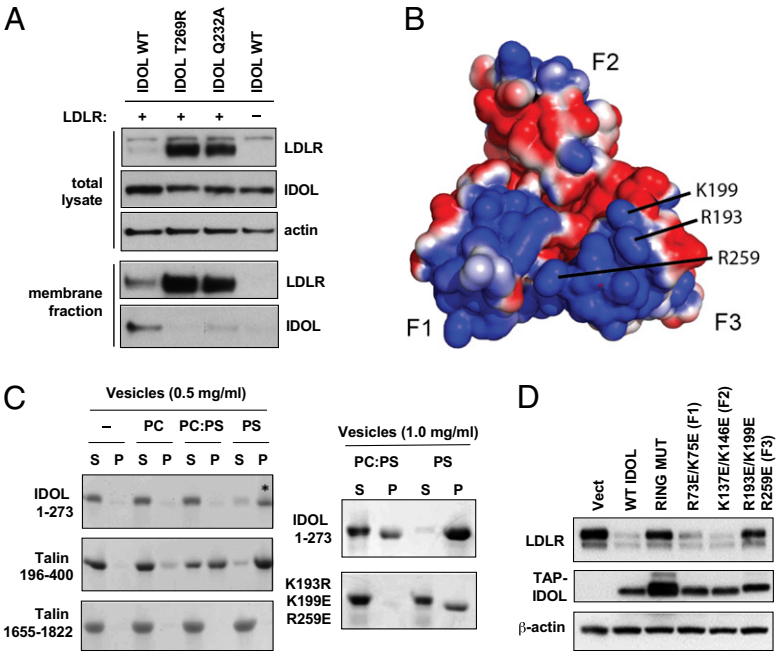


**Fig. 6.** Tripartite FERM–LDLR–membrane interaction is required for IDOL-dependent degradation. (*A*) IDOL association with the LDLR in membrane fractions. HEK293T cells were transfected with vector or LDLR and TAP-IDOL constructs. Membrane fractions were obtained after permeabilization with digitonin (0.05%). *Upper*: Immunoblot of whole-cell lysate inputs. *Lower*: Membrane pellets. (*B*) 3D modeling of the electrostatic surface of the IDOL FERM domain denoting key F3 residues involved in membrane interaction; the basic surfaces are shown in blue and the acidic in red. (*C*) The FERM domain interacts with negatively charged phospholipids. IDOL 1–273 (0.15 mg/mL) was mixed with vesicles (0.5 mg/mL or 1.0 mg/mL) consisting of phosphatidylcholine (PC), phosphatidylserine (PS), or a 4:1 ratio of PC:PS and then centrifuged. Talin 196–400 was used as a positive control and Talin 1655–1822 as a negative control (16). (*D*) Immunoblot of HEK293T lysates after cotransfection with LDLR and IDOL constructs.

deficit (Fig. 6*D*). Importantly, efficient vesicle cosedimentation also required these F3 residues (Fig. 6*C*).

**IDOL FERM Domain Binds Lipoprotein Receptors Tails.** To test whether there is a direct interaction between IDOL and its targets, we used a fluorescence polarization assay to monitor binding of the IDOL FERM domain to a synthetic LDLR peptide. We observed specific binding of the FERM domain to the LDLR but not to a control scrambled peptide. The interaction fit a single-site binding model (Fig. 7*A*). Furthermore, the dissociation constants of the LDLR tail for 1–273 (F1–F3b) and 1–344 (F1–F3c) FERM proteins were comparable, consistent with our data predicting that F3b harbors the primary interaction interface. The dissociation constants for the interactions with FERM 1–273 and 1–344 were 26 μM and 15 μM, respectively. Although this is a relatively weak interaction, it is nevertheless relatively tight compared with other FERM domain interactions (16). Comparable binding affinities were also observed with VLDLR and ApoER2 peptides (18 μM and 8 μM). To confirm the sequence specificity of binding, we introduced mutations suggested by our structural modeling studies to be critical for the interaction. A peptide with a mutation of the VLDLR residue corresponding to LDLR F823 (F832A) showed only a modest reduction in binding affinity, whereas the W822A mutant showed a marked reduction (Fig. 7*B*). Combining these mutations had an additive effect. These data suggest that the hydrophobic interactions of the tryptophan and phenylalanine residues with the FERM are the key determinants of binding affinity. Together, our results indicate that the IDOL FERM mediates direct interactions with negatively charged membrane surfaces and with the cytoplasmic domains of its targets, and that both interactions are required for biological function.

## Discussion

The mechanism by which IDOL specifically targets lipoprotein receptors has not been elucidated. A central unresolved question has been whether IDOL interacts directly with receptor tails or whether its primary target is an intermediate protein. Because IDOL is the only E3 ligase that contains a FERM domain, we postulated that this domain was responsible for target recognition. We show here that the IDOL FERM domain in fact binds directly to LDLR, VLDLR, and ApoER2. Structural modeling and mutagenesis revealed that the F3b subdomain harbors critical residues for target recognition. This subdomain does not align with other FERM sequences, and thus the structural basis for IDOL target recognition is unusual among FERM proteins. Until now, the sequence recognized by IDOL in its targets has also remained elusive. We showed that the F3b subdomain recognizes

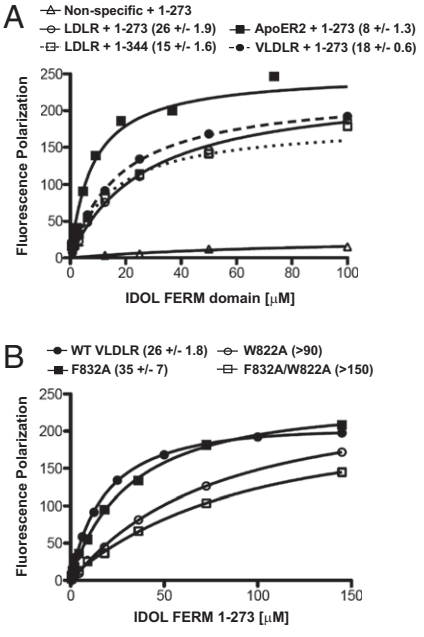


**Fig. 7.** Idol FERM domain binds the cytoplasmic tails of lipoprotein receptors in a sequence-specific manner. (*A*) Fluorescence polarization assay of the binding of BODIPY-labeled $LDLR_{811–833}$ (CKNWRLKNINSINFDNPVYQKTTE), $VLDLR_{820–842}$ (CRNWQHKNMKSMNFDNPVYLKTTE), $ApoER2_{849–871}$ (CRNWKRKNTKSMNFDNPVYRKTTE), or control peptide (CPRPLKEGSITQGTPLKYDTG) to $His_6$-tagged IDOL constructs 1–273 or 1–344. The binding curves were analyzed using GraphPad Prism. (*B*) Fluorescence polarization assay of the binding of BODIPY-labeled WT or mutant VLDLR peptides to $His_6$-tagged IDOL 1–273. Dissociation constants ± SE (μM) for the interactions are indicated in the legend.

the sequence WxxKNxxSI/MxF N-terminal to the NPxY motif; this sequence is unique to LDLR, VLDLR, and ApoER2.

Our data support the importance of the −15 and −5 position (relative to the NPxY motif) for IDOL target recognition. In the model there is a pocket in the IDOL F3b subdomain adjacent to critical amino acids required for target degradation (Y265 and T269) that accommodates the −5 phenylalanine of LDLR, VLDLR, and ApoER2. The surface on IDOL around this pocket is largely nonpolar, and we propose that this surface mediates key interactions with LDLR I821 and W813. The critical role of W813 suggests that the LDLR:IDOL interaction is unusual among FERM domains, because the tryptophan is closer to the membrane than has been seen in other complexes. The fact that mutation of F823 severely reduced LDLR degradation but had only a modest effect on binding suggests that the primary function of this residue may be to optimally position the LDLR tail for ubiquitination by the RING domain.

Despite the fact that ARH readily associates with LDLR tail in biochemical assays (17), IDOL does not. This led us to hypothesize that the cell membrane was a key component of IDOL–receptor interactions. Indeed, IDOL interacts with phospholipid membranes, and we defined positively charged residues on the membrane-facing FERM surface important for this interaction. Because the affinity between IDOL and the LDLR is relatively weak, simultaneous membrane interaction likely provides stability to the complex. In addition, by helping IDOL to localize with its targets, membrane association imparts a spatial constraint on IDOL-dependent degradation. It is also likely that the membrane interaction positions IDOL in the correct orientation to bind lipoprotein receptor tails. Finally, because recent work has indicated that the IDOL RING domain is a functional dimer (18), bivalent IDOL may act to cluster LDLRs on the plasma membrane (Fig. S6).

Although LXRs are not present in organisms lower than vertebrates, the IDOL pathway for lipoprotein receptor degradation is conserved in insects. The same molecular strategy used by IDOL for recognition of the LDLR is used by DNR1 to bind the insect LpR. Key residues predicted by our structural modeling to be involved in FERM–receptor interactions are conserved between IDOL and DNR1. Furthermore, the IDOL recognition sequence is conserved in LDLR, ApoER2, and VLDLR and largely conserved in LpR. Thus, the IDOL FERM–LDLR interaction represents an ancient mechanism for the posttranslational control of lipoprotein receptor activity.

In summary, these studies provide mechanistic insight into sterol-dependent regulation of lipoprotein receptor expression. Proper recognition of both membrane and lipoprotein receptor tails by the IDOL FERM domain is critical for target ubiquitination by the RING domain. These findings, coupled with recent links between IDOL and human cholesterol levels (19), raise the possibility that the FERM–LDLR interaction might be a tractable target for the pharmacologic manipulation of lipid metabolism.

## Methods

**Cell Culture and Transfections.** Cells were maintained in DMEM supplemented with 10% FBS (Omega Scientific) unless otherwise specified. IDOL$^{-/-}$ and LDLR$^{-/-}$ MEFs were immortalized by the SV40 Large T antigen retrovirus and selection with hygromycin B. Stable expression of control retrovirus (pBabe) or IDOL or LDLR constructs was performed as described (8). hApoER2, dDNR1, and dLpR (Open Biosystems) and hVLDLR were cloned into tagged vectors using gateway technology (Invitrogen). All other constructs were previously described (8). Mutations were introduced using the Quickchange site-directed mutagenesis kit (Stratagene) and verified by DNA sequencing. Transfections were performed using Fugene (Roche Diagnostics) according to the manufacturer's instructions with a receptor:IDOL ratio of 4:1 or 2:1. Cells were harvested 24–48 h after transfection.

**Immunoblotting, Biotinylation, Immunoprecipitation, and Fractionation.** HEK293T cells were harvested in RIPA buffer (Boston Bioproducts) supplemented with protease inhibitors (Roche Diagnostics). Lysates were clarified by centrifugation, then quantified using the Bradford assay (Bio-Rad). Proteins were separated on Nupage Bis-Tris gels, then transferred to PVDF (GE Osmonics). Membranes were probed with antibodies against LDLR (Cayman Chemical), V5 (Invitrogen), FLAG (Sigma), HA (Covance), α-tubulin (Calbiochem), β-actin (Sigma), and pan-cadherin (Santa Cruz). HRP-conjugated secondary antibodies (Invitrogen, Bio-Rad) were visualized with chemiluminescence (Amersham). To assess cell surface expression, samples were biotinylated as described (11). For TAP-IDOL immunoprecipitation, lysate treated with MG-132 (25 μM) was incubated with streptactin beads (IBA) overnight with rotation. Samples were washed and heated to 70 °C in 2× sample before immunoblotting. Membrane permeabilization was performed by incubating cells with digitonin (0.05%) at 4 °C for 1 h and centrifugation at 3,000 × *g* for 1 min.

**ACKNOWLEDGMENTS.** We thank N. Zelcer for generation of reagents and valuable discussions in the early stages of this project, and P. Ting, and P. Watson for technical assistance. A.C.C. is funded by National Heart Foundation of Australia Overseas Fellowship O08M3934. B.T.G., L.F., J.W.R.S., and P.T. by Wellcome Trust Grants WT091820 and WT085408. P.T. is a Howard Hughes Medical Institute Investigator and was also supported by National Institutes of Health Grants HL066088 and HL030568.

1. Brown MS, Goldstein JL (1986) A receptor-mediated pathway for cholesterol homeostasis. *Science* 232:34–47.
2. Tolleshaug H, Hobgood KK, Brown MS, Goldstein JL (1983) The LDL receptor locus in familial hypercholesterolemia: Multiple mutations disrupt transport and processing of a membrane receptor. *Cell* 32:941–951.
3. Hobbs HH, Russell DW, Brown MS, Goldstein JL (1990) The LDL receptor locus in familial hypercholesterolemia: Mutational analysis of a membrane protein. *Annu Rev Genet* 24:133–170.
4. Hua X, et al. (1993) SREBP-2, a second basic-helix-loop-helix-leucine zipper protein that stimulates transcription by binding to a sterol regulatory element. *Proc Natl Acad Sci USA* 90:11603–11607.
5. Maxwell KN, Breslow JL (2004) Adenoviral-mediated expression of Pcsk9 in mice results in a low-density lipoprotein receptor knockout phenotype. *Proc Natl Acad Sci USA* 101:7100–7105.
6. Park SW, Moon YA, Horton JD (2004) Post-transcriptional regulation of low density lipoprotein receptor protein by proprotein convertase subtilisin/kexin type 9a in mouse liver. *J Biol Chem* 279:50630–50638.
7. Abifadel M, et al. (2003) Mutations in PCSK9 cause autosomal dominant hypercholesterolemia. *Nat Genet* 34:154–156.
8. Zelcer N, Hong C, Boyadjian R, Tontonoz P (2009) LXR regulates cholesterol uptake through Idol-dependent ubiquitination of the LDL receptor. *Science* 325:100–104.
9. Pearson MA, Reczek D, Bretscher A, Karplus PA (2000) Structure of the ERM protein moesin reveals the FERM domain fold masked by an extended actin binding tail domain. *Cell* 101:259–270.
10. Bornhauser BC, Johansson C, Lindholm D (2003) Functional activities and cellular localization of the ezrin, radixin, moesin (ERM) and RING zinc finger domains in MIR. *FEBS Lett* 553:195–199.
11. Scotti E, et al. (2011) Targeted disruption of the idol gene alters cellular regulation of the low-density lipoprotein receptor by sterols and liver x receptor agonists. *Mol Cell Biol* 31:1885–1893.
12. Di Paolo G, et al. (2002) Recruitment and regulation of phosphatidylinositol phosphate kinase type 1 gamma by the FERM domain of talin. *Nature* 420:85–89.
13. Calderwood DA, et al. (1999) The Talin head domain binds to integrin beta subunit cytoplasmic tails and regulates integrin activation. *J Biol Chem* 274:28071–28074.
14. Wegener KL, et al. (2008) Structural basis for the interaction between the cytoplasmic domain of the hyaluronate receptor layilin and the talin F3 subdomain. *J Mol Biol* 382:112–126.
15. Hong C, et al. (2010) The E3 ubiquitin ligase IDOL induces the degradation of the low density lipoprotein receptor family members VLDLR and ApoER2. *J Biol Chem* 285: 19720–19726.
16. Anthis NJ, et al. (2009) The structure of an integrin/talin complex reveals the basis of inside-out signal transduction. *EMBO J* 28:3623–3632.
17. He G, et al. (2002) ARH is a modular adaptor protein that interacts with the LDL receptor, clathrin, and AP-2. *J Biol Chem* 277:44044–44049.
18. Zhang L, et al. (2011) The IDOL-UBE2D complex mediates sterol-dependent degradation of the LDL receptor. *Genes Dev* 25:1262–1274.
19. Weissglas-Volkov D, et al. (2011) The N342S MYLIP polymorphism is associated with high total cholesterol and increased LDL receptor degradation in humans. *J Clin Invest* 121:3062–3071.